Chapter Three

FERMAT'S PRINCIPLE AND ITS APPLICATIONS

Now in the further development of science, we want more than just a formula. First we have an observation, then we have numbers that we measure, then we have a law which summarizes all the numbers. But the real ***glory*** *of science is that* ***we can find a way of thinking*** *such that the law is* ***evident****. The first way of thinking that made the law about the behavior of light evident was discovered by Fermat in about 1650, and it is called* ***the principle of least time****, or* ***Fermat's principle****.*

—Richard Feynman in *Feynman Lectures on Physics*, Vol. I

Learning Objectives

After reading this chapter, the reader should be able to:

LO 1: state Fermat's principle and its modified version.
LO 2: derive laws of reflection and refraction from Fermat's principle.
LO 3: describe various phenomena by solving the ray equation.
LO 4: obtain ray paths in inhomogeneous media.
LO 5: calculate the time taken by the rays in propagating through a parabolic index medium.

Important Milestones

140 AD — *Greek physicist Claudius Ptolemy measured the angle of refraction in water for different angles of incidence in air and tabulated it.*

1621 — *Although the above-mentioned numerical table was made in 140 AD, it was only in 1621 that Willebrord Snell, a Dutch mathematician, discovered the law of refraction which is now known as Snell's law.*

1637 — *Descartes derived Snell's law; his derivation assumed corpuscular model of light.*

1657 — *Pierre de Fermat enunciated his principle of 'least time' and derived Snell's law of refraction and showed that if the velocity of light in the second medium is less, the ray would bend towards the normal, contrary to what is predicted by the 'corpuscular theory'.*

3.1 INTRODUCTION LO 1

The study of the propagation of light in the realm of geometrical optics employs the concept of rays. To understand what a ray is, consider a circular aperture in front of a point source P as shown in Fig. 3.1. When the diameter of the aperture is quite large (~ 1 cm), then on the screen SS', one can see a patch of light with well-defined boundaries. When we start decreasing the size of the aperture, then at first the size of the patch starts decreasing, but when the size of the aperture becomes very small ($\lesssim$ 0.1 mm) then the pattern obtained on SS' ceases to have well-defined boundaries. This phenomenon is known as diffraction and is a direct consequence of the finiteness of the wavelength (which is denoted by λ). In Chapters 18, 19 and 20 we will discuss the phenomenon of diffraction in great detail and will show that the diffraction effects become smaller with the decrease in wavelength and indeed in the limit of $\lambda \to 0$, the diffraction effects will be absent, and even for extremely small diameters of the aperture, we will obtain a well-defined

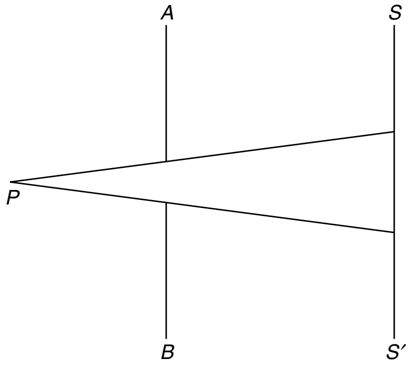

Fig. 3.1 The light emitted by the point source P is allowed to pass through a circular hole and if the diameter of the hole is very large compared to the wavelength of light, then the light patch on the screen SS' has well-defined boundaries.

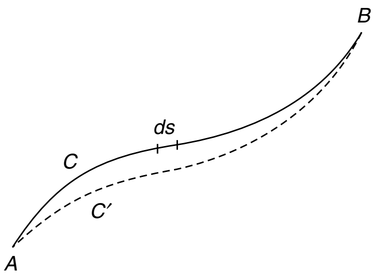

Fig. 3.2 If the path ACB represents the actual ray path then the time taken in traversing the path ACB will be an extremum in comparison to any nearby path $AC'B$.

shadow on the screen SS'. Therefore, in the zero wavelength limit one can obtain an infinitesimally thin pencil of light; this is called a *ray*. Thus, a ray defines the path of propagation of the energy in the limit of the wavelength going to zero. Since light has a wavelength of the order of 10^{-5} cm, which is small compared to the dimensions of normal optical instruments like lenses, mirrors, etc., one can, in many applications, neglect the finiteness of the wavelength. The field of optics under such an approximation (i.e., the neglect of the finiteness of the wavelength) is called geometrical optics.

The field of geometrical optics can be studied by using Fermat's principle which determines the path of the rays. According to this principle, *the ray will correspond to that path for which the time taken is an extremum in comparison to nearby paths*, i.e., it is either a minimum or a maximum or stationary*. Let $n(x, y, z)$ represent the position-dependent refractive index. Then

$$\frac{ds}{c/n} = \frac{n\,ds}{c}$$

will represent the time taken to traverse the geometric path ds in a medium of refractive index n. Here, c represents the speed of light in free space. Thus, if τ represents the total time taken by the ray to traverse the path AB along the curve C (see Fig. 3.2) then

$$\tau = \frac{1}{c}\sum_i n_i\, ds_i = \frac{1}{c}\int_{A \xrightarrow[C]{} B} n\, ds \qquad \textbf{(3.1)}$$

where ds_i represents the i^{th} arc length and n_i the corresponding refractive index; the symbol $A \xrightarrow[C]{} B$ below the integral represents the fact that the integration is from the point A to B through the curve C. Let τ' be the time taken along the nearby path $AC'B$ (shown as the dashed curve in Fig. 3.2), and if ACB indeed represents the path of a ray, then τ will be either less than, greater than or equal to τ' for *all* nearby paths like $AC'B$. Thus according to Fermat's principle, out of the many paths connecting the two points, the light ray would follow that path for which the time taken is an extremum. Since c is a constant, one can alternatively define a ray as the path for which

$$\int_{A \xrightarrow[C]{} B} n\, ds \qquad \textbf{(3.2)}$$

is an extremum**; the above integral represents the optical path from A to B along C; i.e., the ray would follow the path for which

$$\delta \int_{A \to B} n\, ds = 0 \qquad \textbf{(3.3)}$$

where the left-hand side represents the change in the value of the integral due to an infinitesimal variation of the ray path. We may mention here that according to the original statement of Fermat:

> *The actual path between two points taken by a beam of light is the one which is traversed in the least time.*

The above statement is incomplete and slightly incorrect. The correct form is:

> *The actual ray path between two points is the one for which the optical path length is stationary with respect to variations of the path.*

This is expressed by Eq. (3.3) and in this formulation, the ray paths may be maxima, minima or stationary.

From the above principle one can immediately see that in a homogenous medium (i.e., in a medium whose refractive

* The entire field of classical optics (both geometrical and physical) can be understood from Maxwell's equations, and of course, Fermat's principle can be derived from Maxwell's equations (see Refs. 3.1 and 3.2).

** A nice discussion on the extremum principle has been given in Chapter 26 of Ref. 3.3.

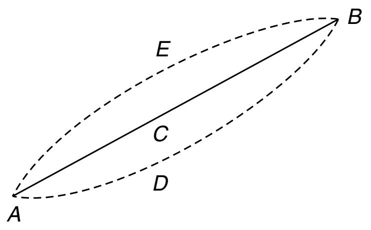

Fig. 3.3 Since the shortest distance between two points is along a straight line, light rays in a homogenous medium are straight lines; all nearby paths like *AEB* or *ADB* will take longer times.

index is constant at each point), the rays will be straight lines because a straight line will correspond to a minimum value of the optical path connecting two points in the medium. Thus referring to Fig. 3.3, if A and B are two points in a homogenous medium, then the ray path will be along the straight line *ACB* because any nearby path like *ADB* or *AEB* will correspond to a longer optical path.

3.2 LAWS OF REFLECTION AND REFRACTION FROM FERMAT'S PRINCIPLE LO 2

To obtain the laws of reflection and refraction from Fermat's principle, consider a plane mirror *MN* as shown in Fig. 3.4. We have to determine the path from *A* to *B* (via the mirror) which has the minimum optical path length. Since the path would lie completely in a homogenous medium, we need to minimize only the path length. Thus we have to find that path *APB* for which $AP + PB$ is a minimum. To find the position of *P* on the mirror, we drop a perpendicular from *A* on the mirror and let *A′* be a point on the perpendicular such that $AR = RA'$; thus $AP = PA'$ and $AQ = A'Q$ where *AQB* is another path adjacent to *APB*. Thus we have to minimize the length *A′PB*. Clearly, for *A′PB* to be a minimum, *P* must be on the straight line *A′B*. Thus, the points *A*, *A′*, *P* and *B* will be in the same plane and if we draw a normal *PS* at *P* then this normal will also lie in the same plane. Simple geometric considerations show that

$$\angle APS = \angle SPB$$

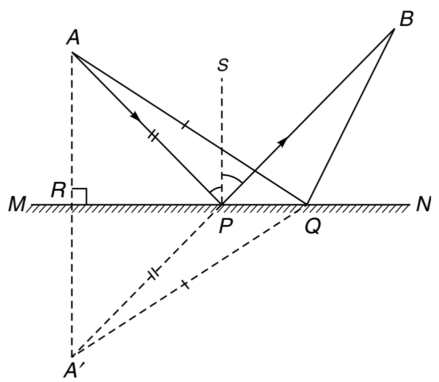

Fig. 3.4 The shortest path connecting the two points *A* and *B* via the mirror is along the path *APB* where the point *P* is such that *AP*, *PS* and *PB* are in the same plane and $\angle APS = \angle SPB$; *PS* being the normal to the plane of the mirror. The straight line path *AB* is *also* a ray.

Thus for minimum optical path length, the angle of incidence $i(= \angle APS)$ and the angle of reflection $r\ (= \angle SPB)$ must be equal and the incident ray, the reflected ray and the normal to the surface at the point of incidence on the mirror must be in the same plane. These form the laws of reflection. It should be pointed out that, in the presence of the mirror there will be two ray paths which will connect the points *A* and *B*; the two paths will be *AB* and *APB*. Fermat's principle tells us that whenever the optical path length is an extremum, we will have a ray, and thus, in general, there may be more than one ray path connecting two points.

To obtain the laws of refraction, let *PQ* be a surface separating two media of refractive indices n_1 and n_2 as shown in Fig. 3.5. Let a ray starting from the point *A*, intersect the interface at *R* and proceed to *B* along *RB*. Clearly, for minimum optical path length, the incident ray, the refracted ray and the normal to the interface must all lie in the same plane. To determine that point *R* for which the optical path length from *A* to *B* is a minimum, we drop perpendiculars *AM* and *BN* from *A* and *B* respectively on the interface *PQ*. Let $AM = h_1$, $BN = h_2$ and $MR = x$. Then since *A* and *B* are fixed, $RN = L - x$, where $MN = L$ is a fixed quantity. The optical path length from *A* to *B*, by definition, is

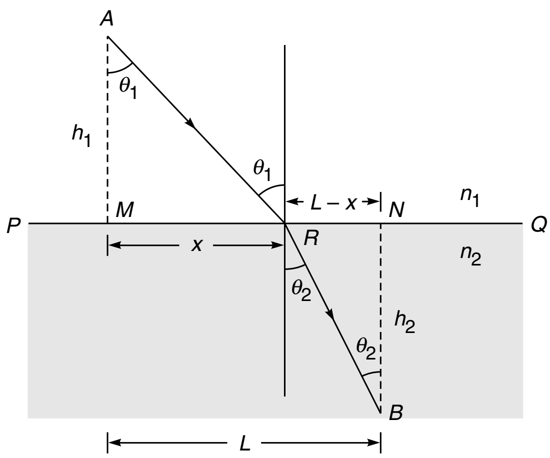

Fig. 3.5 *A* and *B* are two points in media of refractive indices n_1 and n_2. The ray path connecting *A* and *B* will be such that $n_1 \sin \theta_1 = n_2 \sin \theta_2$.

$$L_{op} = n_1\, AR + n_2\, RB$$
$$= n_1 \sqrt{x^2 + h_1^2} + n_2 \sqrt{(L-x)^2 + h_2^2} \qquad \textbf{(3.4)}$$

To minimize this, we must have

$$\frac{dL_{op}}{dx} = 0$$

i.e.,
$$\frac{n_1 x}{\sqrt{x^2 + h_1^2}} - \frac{n_2 (L-x)}{\sqrt{(L-x)^2 + h_2^2}} = 0 \qquad \textbf{(3.5)}$$

Further, as can be seen from Fig. 3.5

$$\sin\theta_1 = \frac{x}{\sqrt{x^2 + h_1^2}}$$

and
$$\sin\theta_2 = \frac{(L-x)}{\sqrt{(L-x)^2 + h_2^2}}$$

Thus, Eq. (3.5) becomes

$$n_1 \sin\theta_1 = n_1 \sin\theta_2 \qquad \textbf{(3.6)}$$

which is the Snell's law of refraction.

The laws of reflection and refraction form the basic laws for tracing light rays through simple optical systems, like a system of lenses and mirrors, etc.

Example 3.1 Consider a set of rays, parallel to the axis, incident on a paraboloidal reflector (see Fig. 3.6). Show by using Fermat's principle, that all the rays will pass through the focus of the paraboloid; a paraboloid is obtained by rotating a parabola about its axis. This is the reason why a paraboloidal reflector is used to focus parallel rays from a distant source, like in radio astronomy (see Figs. 3.7 and 3.8).

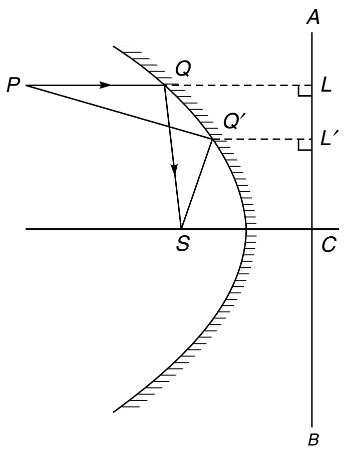

Fig. 3.6 All rays parallel to the axis of a paraboloidal reflector pass through the focus after reflection (the line *ACB* is the directrix). It is for this reason that antennas (for collecting electromagnetic waves) or solar collectors are often paraboloidal in shape.

Fig. 3.7 A paraboloidal satellite dish. [*Photograph courtesy: McGraw-Hill Digital Access Library. A color photograph of the above figure appears as Fig. 1 in the prelim pages*].

Fig. 3.8 Fully steerable 45 m paraboloidal dishes of the Giant Metrewave Radio Telescope (GMRT) in Pune, India. The GMRT consists of 30 dishes of 45 m diameter with 14 antennas in the Central Array. [*Photograph courtesy: Professor Govind Swarup, GMRT, Pune. A color photograph of the above figure appears as Fig. 2 in the prelim pages*].

Solution: Consider a ray *PQ*, parallel to the axis of the parabola, incident at the point *Q* (see Fig. 3.6). In order to find the reflected ray, one has to draw a normal at the point *Q* and then draw the reflected ray. It can be shown from geometrical considerations that the reflected ray *QS* will always pass through the focus *S*. However, this procedure will be quite cumbersome and as we will show, the use of Fermat's principle leads us to the desired results immediately.

To use Fermat's principle, we try to find out the ray connecting the focus *S* and an arbitrary point *P* (see Fig. 3.6). Let the ray path be *PQ′S*. According to Fermat's principle, the ray path will correspond to a minimum value of $PQ' + Q'S$. From the point Q' we drop a perpendicular $Q'L'$, on the directrix *AB*. From the definition of the parabola it follows that $Q'L' = Q'S$. Thus,

$$PQ' + Q'S = PQ' + Q'L'$$

Let L be the foot of the perpendicular drawn from the point P on AB. Then, for $PQ' + Q'L'$ to be a minimum, the point Q should lie on the straight line PQL, and thus the actual ray which connects the points P and S will be $PQ + QS$ where PQ is parallel to the axis. Therefore, all rays parallel to the axis will pass through S and conversely, all rays emanating from the point S will become parallel to the axis after suffering a reflection.

Example 3.2 Consider an elliptical reflector whose foci are the points S_1 and S_2 (see Fig. 3.9). Show that all rays emanating from the point S_1 will pass through the point S_2 after undergoing a reflection.

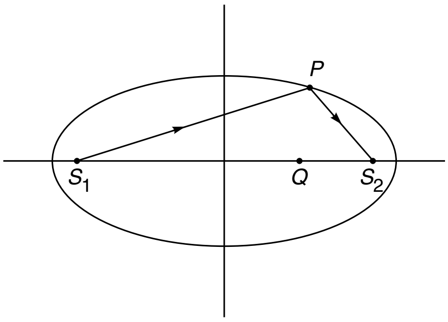

Fig. 3.9 All rays emanating from one of the foci of an ellipsoidal reflector will pass through the other focus.

Solution: Consider an arbitrary point P on the ellipse (see Fig. 3.9). It is well known that $S_1P + S_2P$ is a constant and therefore, all rays emanating from the point S_1 will pass through S_2. (Notice that here we have an example where the time taken by the ray is stationary, i.e., it is neither a maximum nor a minimum but has a constant value for all points lying on the mirror.) As a corollary, we may note the following two points:

(a) Excepting the rays along the axis, no other ray (emanating from either of the foci) will pass through an arbitrary point Q which lies on the axis.

(b) The above considerations will remain valid even for an ellipsoid of revolution obtained by rotating the ellipse about its major axis.

Because of the above-mentioned property of elliptical reflectors, they are often used in laser systems. For example, in a ruby laser (see Sec. 27.3) one may have a configuration in which the laser rod and the flash lamp coincide with the focal lines of a cylindrical reflector of elliptical cross section; such a configuration leads to an efficient transfer of energy from the lamp to the ruby rod.

Example 3.3 Consider a spherical refracting surface SPM separating two media of refractive indices n_1 and n_2 (see Fig. 3.10). The point C represents the center of the spherical surface SPM. Consider two points O and Q such that the points O, C and Q are in a straight line. Calculate the optical path length OSQ in terms of the distances x, y, r and the angle θ (see Fig. 3.10). Use Fermat's principle to find the ray connecting the two points O and Q. Also, assuming the angle θ to be small, determine the paraxial image of the point O.

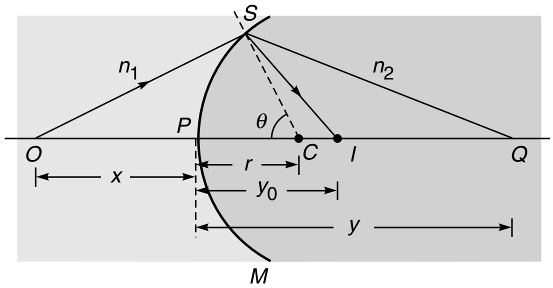

Fig. 3.10 SPM is a spherical refracting surface separating two media of refractive indices n_1 and n_2. C represents the center of the spherical surface.

[*Note*: We reserve the symbol R to represent the radius of curvature of a spherical surface which will be positive (or negative) depending upon whether the center of curvature lies on the right (or left) of the point P. The quantity r represents the magnitude of the radius of curvature which, for Fig. 3.10, happens to be R. Similarly, the quantities x and y are the magnitudes of the distances; the sign convention is discussed later on in this problem.]

Solution: From the triangle SOC, we have

$$OS = [(x + r)^2 + r^2 - 2(x + r)\, r \cos\theta]^{1/2}$$

$$\approx \left[x^2 + 2rx + 2r^2 - 2(xr + r^2)\left(1 - \frac{\theta^2}{2}\right)\right]^{1/2}$$

$$\approx x\left[1 + \frac{rx + r^2}{x^2}\theta^2\right]^{1/2} \approx x + \frac{1}{2}r^2\left(\frac{1}{r} + \frac{1}{x}\right)\theta^2$$

where we have assumed θ (measured in radians) to be small so that we may use the expression

$$\cos\theta \approx 1 - \frac{\theta^2}{2}$$

and also make a binomial expansion. Similarly, by considering the triangle SCQ, we would have

$$SQ \approx y - \frac{1}{2}r^2\left(\frac{1}{r} - \frac{1}{y}\right)\theta^2$$

Thus the optical path length OSQ is given by

$$L_{\text{op}} = n_1\, OS + n_2\, SQ$$

$$\approx (n_1 x + n_2 y) + \frac{1}{2}r^2\left[\frac{n_1}{x} + \frac{n_2}{y} - \frac{n_2 - n_1}{r}\right]\theta^2 \tag{3.7}$$

For the optical path to be an extremum we must have

$$\frac{dL_{\text{op}}}{d\theta} = 0 = r^2\left[\frac{n_1}{x} + \frac{n_2}{y} - \frac{n_2 - n_1}{r}\right]\theta \tag{3.8}$$

Thus, unless the quantity inside the square brackets is zero we must have $\theta = 0$ implying that the *only* ray connecting the points O and Q will be the straight line path OPQ which also follows from Snell's law because the ray OP hits the spherical surface normally and should proceed undeviated.

On the other hand, if the value of y was such that the quantity inside the square brackets was zero, i.e., if y was equal to y_0 such that

$$\frac{n_2}{y_0} + \frac{n_1}{x} = \frac{n_2 - n_1}{r} \tag{3.9}$$

then $dL_{op}/d\theta$ would vanish for *all* values of θ; of course, θ is assumed to be small—which is the paraxial approximation. Now, if the point I corresponds to $PI = y_0$ (see Fig. 3.10) then *all* paths like OSI are allowed ray paths implying that *all* (paraxial) rays emanating from O will pass through I and I will, therefore represent the paraxial image point. Obviously, all rays like OSI (which start from O and pass through I) take the *same* amount of time in reaching the point I.

We should mention that Eq. (3.9) is a particular form of the equation determining the paraxial image point

$$\frac{n_2}{v} - \frac{n_1}{u} = \frac{n_2 - n_1}{R} \tag{3.10}$$

with the sign convention that all distances measured to the right of the point P are positive and those to its left negative. Thus $u = -x$, $v = +y$ and $r = +R$.

In order to determine whether the ray path OPQ corresponds to minimum time or maximum time or stationary, we must determine the sign of $d^2L_{op}/d\theta^2$ which is given by

$$\frac{d^2L_{op}}{d\theta^2} = r^2\left[\frac{n_1}{x} + \frac{n_2}{y} - \frac{n_2 - n_1}{r}\right]$$

$$= r^2 n_2 \left[\frac{1}{y} - \frac{1}{y_0}\right]$$

Obviously, if $y > y_0$ (i.e., the point Q is on the right of the paraxial image point I) $d^2L_{op}/d\theta^2$ is negative and the ray path OPQ corresponds to *maximum* time in comparison with nearby paths and conversely. On the other hand, if $y = y_0$, $d^2L_{op}/d\theta^2$ will vanish implying that the extremum corresponds to stationarity. Thus, in the paraxial approximation, all rays emanating from the point O will take the same amount of time in reaching the point I.

Alternatively, one can argue that if I is the paraxial image point of P then

$$n_1\, OP + n_2\, PI = n_1\, OS + n_2\, SI$$

Thus, when Q lies on the right of the point I, we have

$$\begin{aligned} n_1\, OP + n_2\, PQ &= n_1\, OS + n_2\,(SI - PI + PQ) \\ &= n_1\, OS + n_2\,(SI + IQ) \\ &> n_1\, OS + n_2\, SQ \end{aligned}$$

implying that the ray path OPQ corresponds to a maximum. Similarly, when Q lies on the left of the point I then the ray path OPQ corresponds to a minimum and when Q coincides with I, we have the stationarity condition.

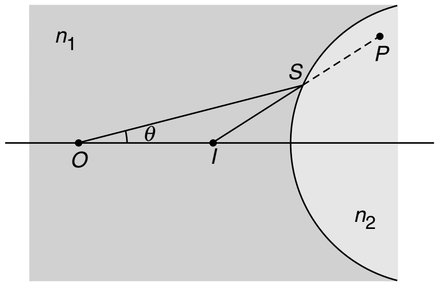

Fig. 3.11 The refracted ray is assumed to diverge away from the principal axis.

Example 3.4 We again consider refraction at a spherical surface; however, the refracted ray is assumed to diverge away from the principal axis (see Fig. 3.11). Let us consider paraxial rays and let I be a point (on the axis) such that $n_1\, OS - n_2\, SI$ is independent of the point S. Thus, for paraxial rays, the quantity

$$n_1\, OS - n_2\, SI \quad \text{is independent of } \theta \tag{3.11}$$

and is an extremum. Let P be an arbitrary point in the second medium and we wish to find the ray path connecting the points O and P. For OSP to be an allowed ray path

$$L_{op} = n_1\, OS + n_2\, SP \text{ should be an extremum}$$

or

$$L_{op} = (n_1\, OS - n_2\, SI) + n_2\,(IS + SP) \text{ should be an extremum}$$

where we have added and subtracted $n_2\, SI$. Now, the point I is such that the first quantity is already an extremum thus, the quantity $SP + SI$ should be an extremum and therefore it should be a straight line. Thus the refracted ray must appear to come from the point I. We may therefore say that for a virtual image, we must make the quantity

$$n_1\, OS - n_2\, SI \tag{3.12}$$

an extremum.

3.3 RAY PATHS IN AN INHOMOGENEOUS MEDIUM

LO 3

In an inhomogeneous medium, the refractive index varies in a continuous manner and, in general, the ray paths are curved. For example, on a hot day, the air near the ground has a higher temperature than the air which is much above the surface. Since the density of air decreases with increase in temperature, the refractive index increases continuously as we go above the ground. This leads to the phenomenon known as *mirage*. We will use Snell's law (or Fermat's principle) to determine the ray paths in an inhomogeneous medium. We will restrict ourselves to the special case when the refractive index changes continuously along one direction only; we assume this direction to be along the x-axis.

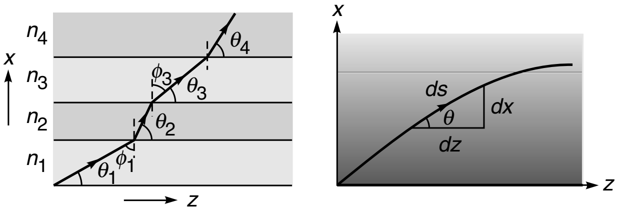

Fig. 3.12 (a) In a layered structure, the ray bends in such a way that the product $n_i \cos \theta_i$ remains constant. (b) For a medium with continuously varying refractive index, the ray path bends in such a way that the product $n(x) \cos \theta(x)$ remains constant.

The inhomogeneous medium can be thought of as a limiting case of a medium consisting of a continuous set of thin slices of media of different refractive indices—see Fig. 3.12(a). At each interface, the light ray satisfies Snell's law and one obtains [see Fig. 3.12(a)]

$$n_1 \sin \phi_1 = n_2 \sin \phi_2 = n_3 \sin \phi_3 = ... \quad \textbf{(3.13)}$$

Thus, we may state that the product

$$n(x) \cos \theta(x) = n(x) \sin \phi(x) \quad \textbf{(3.14)}$$

is an invariant of the ray path; we will denote this invariant by $\tilde{\beta}$. The value of this invariant may be determined from the fact that if the ray initially makes an angle θ_1 (with the z-axis) at a point where the refractive index is n_1, then the value of $\tilde{\beta}$ is $n_1 \cos \theta_1$. Thus, in the limiting case of a continuous variation of refractive index, the piecewise straight lines shown in Fig. 3.12(a) form a continuous curve which is determined from the equation

$$n(x) \cos \theta(x) = n_1 \cos \theta_1 = \tilde{\beta} \quad \textbf{(3.15)}$$

implying that as the refractive index changes, the ray path bends in such a way that the product $n(x) \cos \theta(x)$ remains constant [see Fig. 3.12(b)]. Equation (3.15) can be used to derive the ray equation (see Sec. 3.4).

3.3.1 The Phenomenon of Mirage*

We are now in a position to qualitatively discuss the formation of a mirage. As mentioned earlier, on a hot day the refractive index continuously decreases as we go near the ground. Indeed, the refractive index variation can be approximately assumed to be of the form

$$n(x) \approx n_0 + kx \qquad 0 < x < \text{few meters} \quad \textbf{(3.16)}$$

where n_0 is the refractive index of air at $x = 0$ (i.e., just above the ground) and k is a constant. The exact ray paths (see Example 3.8) are shown in Fig. 3.13.

* For more details, see Refs. 3.4–3.8.

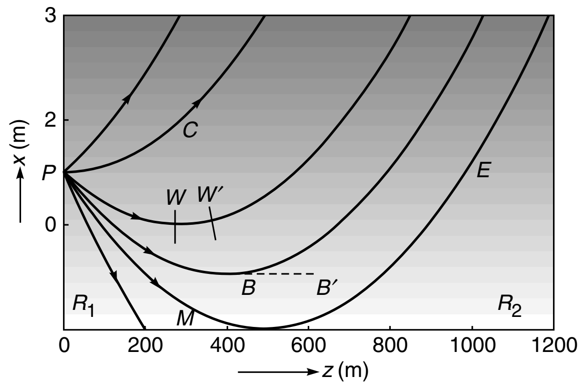

Fig. 3.13 Ray paths in a medium characterized by a linear variation of refractive index [see Eq.(3.16)] with $k \approx 1.234 \times 10^{-5}$ m^{-1}. The object point is at a height of 1.5 m and the curves correspond to +0.2°, 0°, -0.2°, -0.28°, -0.3486° and -0.5° The shading shows that the refractive index increases with x.

We consider a ray which becomes horizontal at $x = 0$. At the eye position E ($x = x_e$), if the refractive index is n_e, and if at that point the ray makes an angle θ_e with the horizontal then

$$\tilde{\beta} = n_0 = n_e \cos \theta_e \quad \textbf{(3.17)}$$

Usually $\theta_e << 1$ so that

$$\frac{n_0}{n_e} = \cos \theta_e \approx 1 - \frac{1}{2}\theta_e^2$$

$$\Rightarrow \qquad \theta_e \approx \sqrt{2\left(1 - \frac{n_0}{n_e}\right)} \quad \textbf{(3.18)}$$

At constant air pressure

$$(n_0 - 1)T_0 \approx (n_e - 1)T_e \quad \textbf{(3.19)}$$

From Eq. (3.19), we get

$$1 - \frac{n_0 - 1}{n_e - 1} = 1 - \frac{T_e}{T_0}$$

or

$$\frac{n_e - n_0}{n_e} = \frac{n_e - 1}{n_e}\left(1 - \frac{T_e}{T_0}\right)$$

so that

$$\theta_e \approx \sqrt{2\left(1 - \frac{1}{n_e}\right)\left(1 - \frac{T_e}{T_0}\right)} \quad \textbf{(3.20)}$$

On a typical hot day, the temperature near road surface $T_0 \approx 323$ K (= 50 °C) and, about 1.5 m above the ground, $T_e \approx 303$ K (= 30 °C). Now, at 30 °C, $n_e \approx 1.00026$ giving

$\theta_e \approx 5.67 \times 10^{-3}$ radians $\approx 0.325°$. In Fig. 3.13, we have shown rays emanating (at different angles) from a point P which is 1.5 m above the ground; thus each ray has a specified value of the invariant $\tilde{\beta}$ (= $n_1 \cos \theta_1$). The figure shows that when the object point P and the observation point E are close to the ground, the only ray path connecting points P and E will be along the curve PME and that a ray emanating horizontally from the point P will propagate in the upward direction as PC as shown in the figure. Thus, in such a condition, the eye at E will see the mirage and *not see* the object directly at P. We also find that there is a region R_2 where none of the rays (emanating from the point P) reaches; thus, an eye in this region can neither see the object nor its image. This is therefore called the *shadow region*. Furthermore, there is also a region R_1 where only the object is directly visible and the virtual image is not seen.

We should mention here that the *bending up* of the ray after it becomes parallel to the z-axis cannot be directly inferred from Eq. (3.15) because at such a point, $\theta = 0$ and one may expect the ray to proceed horizontally beyond the turning point as shown by a dotted line in Fig. 3.13; the point at which $\theta = 0$ is known as the *turning point*. However, from considerations of symmetry and from the reversibility of ray paths, it immediately follows that the ray path should be symmetrical about the turning point and hence bend up. Physically, the bending of the ray can be understood by considering a small portion of a wave front such as W (see Fig. 3.13); the upper edge will travel with a lesser speed in comparison with the lower edge, and this will cause the wave front to tilt (see W') making the ray to bend. Furthermore, a straight line path like BB' does not correspond to an extremum value of the optical path.

We next consider a refractive index variation which saturates to a constant value as $x \rightarrow \infty$:

$$n^2(x) = n_0^2 + n_2^2\,(1 - e^{-\alpha x});\; x > 0 \qquad \textbf{(3.21)}$$

where n_0, n_2 and α are constants and once again, x represents the height above the ground. The refractive index at x = 0 is n_0 and for large values of x, it approaches $(n_0^2 + n_2^2)^{1/2}$. The exact ray paths are obtained by solving the ray equation (see Example 3.10) and are shown in Figs. 3.14 and 3.15; they correspond to the following values of various parameters:

$$n_0 = 1.000233,\; n_2 = 0.45836$$

$$\text{and} \quad \alpha = 2.303 \text{ m}^{-1} \qquad \textbf{(3.22)}$$

The actual values of the refractive index for parameters given by the above equation are not very realistic—nevertheless, it allows us to understand qualitatively the ray paths in a graded index medium. Figures 3.14 and 3.15 show the ray paths emanating from points that are 0.43 m and 2.8 m above the ground respectively. In Fig. 3.14, the point P corresponds to a value of the refractive index equal to 1.06455 (= n_1) and different rays correspond to different values of θ_1, the angle that the ray makes with the z-axis at the point P. From Fig. 3.14 we again see that when the object point P and the observation point E are close to the ground, the only ray path connecting points P and E will be along the curve PME and that a ray emanating horizontally from the point P will propagate in the upward direction, shown as PC in Fig. 3.14. Thus, in such a condition, the eye at E will see the mirage and *not see* the object directly at P. However, if points P and E are much above the ground (see Fig. 3.15), the eye will see the object almost directly (because of rays like PCE) and will also receive rays appearing to emanate from points like P'. It may be readily seen that different rays do not appear to come from the same point and hence the reflected image seen will have considerable aberrations. Once again, there is a *shadow region* R_2 where none of the rays (emanating from the point P) reaches there; thus, an eye in this region can neither see the object nor its image. The actual formation of mirage is shown in Figs. 3.16 and 3.17.

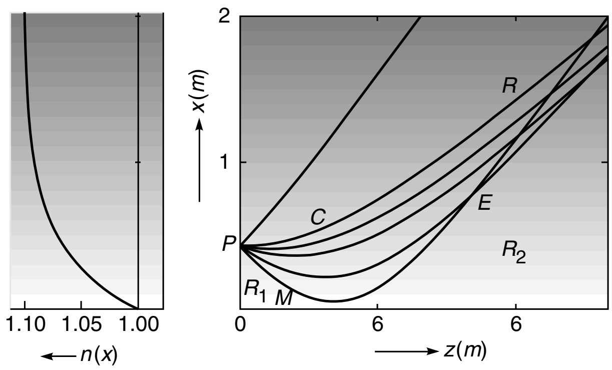

Fig. 3.14 Ray paths in a medium characterized by Eqs. (3.21) and (3.22). The object point is at a height of $1/\alpha$ ($\approx$0.43 m) and the curves correspond to θ_1 (the initial launch angle) = $+\pi/10$, 0, $-\pi/60$, $-\pi/30$, $-\pi/15$ and $-\pi/10$. The shading shows that the refractive index increases with x.

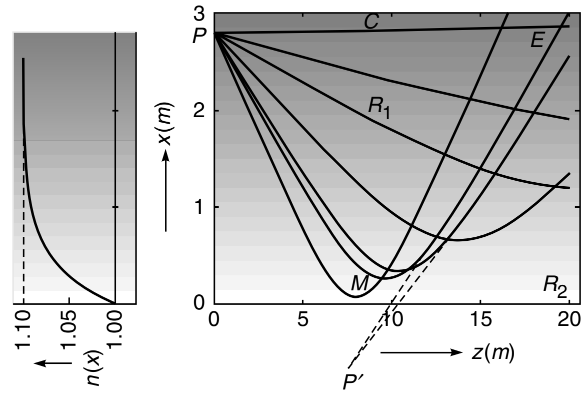

Fig. 3.15 Ray paths in a medium characterized by Eqs. (3.21) and (3.22). The object point is at a height of 2.8 m and the curves correspond to θ_1 (the initial launch angle) = 0, $-\pi/60$, $-\pi/30$, $-\pi/16$, $-\pi/11$, $-\pi/10$ and $-\pi/8$. The shading shows that the refractive index increases with x.

Fig. 3.16 A typical mirage as seen on a hot road on a warm day. [*Photograph adapted from http://fizyka.phys.put.poznan.pl/~pieransk/Physics%20Around%20Us/Air%20mirror.jpg. A color photograph of the above figure appears as Fig. 4 in the prelim pages; used with permission from Professor Piernaski*].

Fig. 3.17 This is actually *not* a reflection in the ocean, but the miraged (inverted) image of the Sun's lower edge. A few seconds later (notice the motion of the bird to the left of the Sun!), the reflection fuses with the erect image. The photographs were taken by Dr. George Kaplan of the U. S. Naval Observatory and are on the Naval Observatory's website. [*Ref: http://mintaka.sdsu.edu/GF/explain/simulations/infmir/Kaplan_ photos.html. A color photograph of the above figure appears as Fig. 3 in the prelim pages. Used with permissions from Dr. Kaplan and Dr. Young*].

Example 3.5 As an example, for an object shown in Fig. 3.14, let us calculate the angle at which the ray should be launched so that it becomes horizontal at $x = 0.2$ m. Now,

$$\text{at } x = 0.2 \text{ m}, \quad n(x) = 1.03827$$

Thus, if θ_1 represents the angle that the ray makes with the z-axis at the point P (see Fig. 3.14) then

$$n_1 \cos \theta_1 = 1.03827 \times \cos 0$$

implying

$$\theta_1 \approx 13°$$

Further, for the ray which becomes horizontal at $x = 0.2$ m the value of the invariant is given by

$$\tilde{\beta} \approx 1.03827$$

Example 3.6 In Fig. 3.15, the object point corresponds to $x = 2.8$ m where $n(x) \approx 1.1$. Thus for a ray launched with $\theta_1 = -\pi/8$,

$$\tilde{\beta} = 1.1 \cos \theta_1 = 1.01627$$

Thus if the ray becomes horizontal at $x = x_2$ then

$$n(x_2) = \tilde{\beta} = 1.01627$$

and

$$x_2 = -\frac{1}{\alpha} \ln\left[1 - \frac{n^2(x_2) - n_0^2}{n_2^2}\right]$$

$$\approx 0.073 \text{ m}$$

3.3.2 The Phenomenon of Looming

The formation of mirage discussed above occurs due to increase in the refractive index of air above the hot surface. On the other hand, above cold sea water, the air near the water surface is colder than the air above it and hence there is an opposite temperature gradient. A suitable refractive index variation for such a case can be written as

$$n^2(x) = n_0^2 + n_2^2\, e^{-\alpha x} \qquad \textbf{(3.23)}$$

The equation describing the ray path is discussed in Problem 3.13. We assume the values of n_0, n_2 and α to be given by Eq. (3.22). For an object point P at a height of 0.5 m, the ray paths are shown in Fig. 3.18. If the eye is at E, then it will receive rays appearing to emanate from P'. Such a phenomenon in which the object appears to be above its actual position is known as *looming*. It is commonly observed in viewing ships over cold sea waters (see Figs. 3.19 and 3.20). Moreover, since no other rays emanating from P reach A, the object cannot be observed directly.

3.3.3 The Graded Index Atmosphere

One of the interesting phenomena associated with imaging in a graded index medium is the non-circular shape of the setting or the rising sun (see Fig. 3.21 and Fig. 9 in the prelim pages). This can easily be understood in the following manner: The refractive index of the air gradually decreases as we move outwards. If we approximate the continuous refractive index gradient by a finite number of layers (each layer having a specific refractive index) then the ray will bend in a way similar to that shown in Fig. 3.22. Thus the sun (which is actually at S) appears to be in the direction of S'. It is for this reason that the setting sun appears flattened and also leads to the

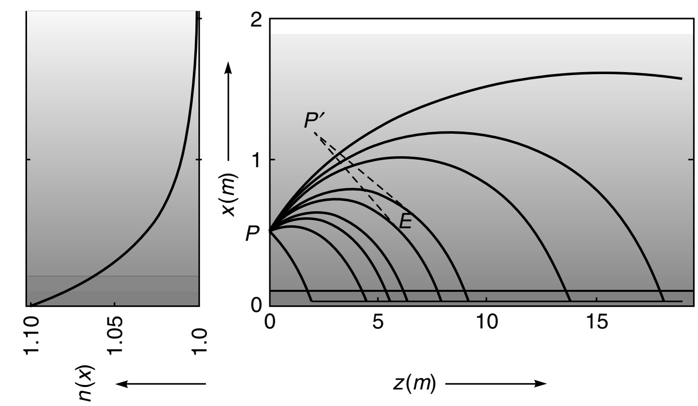

Fig. 3.18 Ray paths corresponding to the refractive index distribution given by Eq. (3.23) for an object at a height of 0.5 m; the values of n_0, n_2 and α are given by Eq. (3.22).

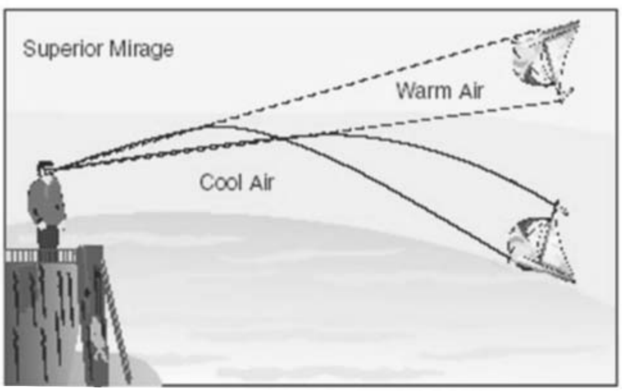

Fig. 3.19 If we are looking at the ocean on a cold day, we find that the air near the surface of the water is cold and it gets warmer as we go up. Thus, as we go up, the refractive index decreases continuously and because of curved ray paths, one will observe an inverted image of the ship (at a greater height) as shown in the figure above; this is known as the *superior mirage*. [*A color photoraph of the above figure appears as Fig. 5 in the prelim pages*].

Fig. 3.20 A house in the archipelago with a superior mirage. [*Figure adapted from http://virtual.finland.fi/netcomm/news/showarticle.asp?intNWSAID=25722. A color photograph of the above figure appears as Fig. 6 in the prelim pages. Used with permission from Dr. P. Parviainen*].

Fig. 3.21 The non-circular shape of the setting sun.

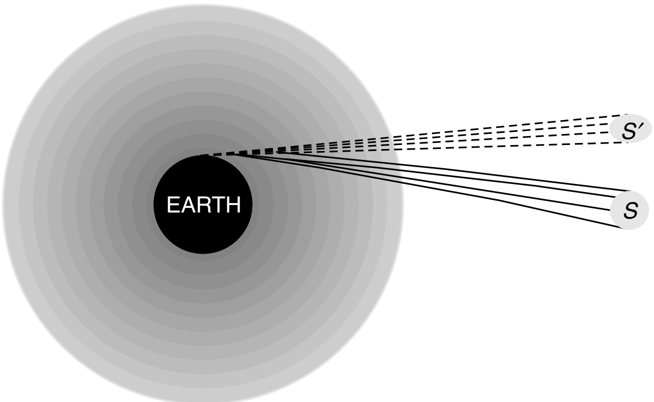

Fig. 3.22 Because of refraction, light from S appears to come from S'.

fact that the days are usually about 5 minutes longer than they would have been in the absence of the atmosphere. Obviously, if we were on the surface of the moon, the rising or the setting sun would not only look white but also circular in shape!

3.4 THE RAY EQUATION AND ITS SOLUTIONS LO 4

In this section, we will derive the ray equation, the solution of which will give the precise ray paths in an inhomogeneous medium. We will restrict ourselves to the special case when the refractive index changes continuously along only one direction, which we assume to be along the x-axis. This medium can be thought of as the limiting case of a medium comprising a continuous set of thin slices of media of different refractive indices. As discussed earlier, for a continuously varying refractive index, the product $n(x) \cos \theta(x)$ is an invariant of the ray path which we denote by $\tilde{\beta}$:

$$n(x) \cos \theta(x) = \tilde{\beta} \tag{3.24}$$

Furthermore, for a continuous variation of refractive index, the piecewise straight lines shown in Fig. 3.12(a) forms a continuous curve as in Fig. 3.12(b). If ds represents the infinitesimal arc length along the curve, then

$$(ds)^2 = (dx)^2 + (dz)^2$$

or

$$\left(\frac{ds}{dz}\right)^2 = \left(\frac{dx}{dz}\right)^2 + 1 \tag{3.25}$$

Now, if we refer to Fig. 3.12(b), we find that

$$\frac{dz}{ds} = \cos \theta = \frac{\tilde{\beta}}{n(x)} \tag{3.26}$$

Thus Eq. (3.25) becomes

$$\left(\frac{dx}{dz}\right)^2 = \frac{n^2(x)}{\tilde{\beta}^2} - 1 \tag{3.27}$$

For a given $n(x)$ variation, Eq. (3.27) can be integrated to give the ray path $x(z)$; however, it is often more convenient to put Eq. (3.27) in a slightly different form by differentiating it with respect to z:

$$2\frac{dx}{dz}\frac{d^2x}{dz^2} = \frac{1}{\tilde{\beta}^2}\frac{dn^2}{dx}\frac{dx}{dz}$$

or

$$\frac{d^2x}{dz^2} = \frac{1}{2\tilde{\beta}^2}\frac{dn^2}{dx} \tag{3.28}$$

Both, Eqs. (3.27) and (3.28), represent rigorously correct ray equations when the refractive index depends only on the x-coordinate.

Example 3.7 As a simple application of Eq. (3.28), let us consider a homogeneous medium for which $n(x)$ is a constant. In such a case, the RHS of Eq. (3.28) is zero and one obtains

$$\frac{d^2x}{dz^2} = 0$$

Integrating the above equation twice with respect to z, we obtain

$$x = Az + B$$

which is the equation of a straight line, as it ought to be in a homogeneous medium.

Example 3.8 We next consider the ray paths in a medium characterized by the following refractive index variation

$$n(x) = n_0 + kx \tag{3.29}$$

For the above profile, the ray equation [Eq. (3.28)] takes the form

$$\frac{d^2x}{dz^2} = \frac{1}{2\tilde{\beta}^2}\frac{dn^2}{dx} = \frac{k}{\tilde{\beta}^2}[n_0 + kx]$$

or

$$\frac{d^2X}{dz^2} = \kappa^2 X(z) \tag{3.30}$$

where

$$X \equiv x + \frac{n_0}{k} \text{ and } \kappa = \frac{k}{\tilde{\beta}} \tag{3.31}$$

Thus the ray path is given by

$$x(z) = -\frac{n_0}{k} + C_1 e^{\kappa z} + C_2 e^{-\kappa z} \tag{3.32}$$

where the constants C_1 and C_2 are to be determined from initial conditions. We assume that at $z = 0$, the ray is launched at $x = x_1$ making an angle θ_1 with the z-axis; thus

$$x(z = 0) = x_1$$

and

$$\left.\frac{dx}{dz}\right|_{z=0} = \tan \theta_1$$

Elementary manipulations would give us

$$C_1 = \frac{1}{2}\left[x_1 + \frac{1}{k}(n_0 + n_1 \sin \theta_1)\right] \tag{3.33}$$

and

$$C_2 = \frac{1}{2}\left[x_1 + \frac{1}{k}(n_0 - n_1 \sin \theta_1)\right] \tag{3.34}$$

where $n_1 = n_0 + kx_1$ represents the refractive index at $x = x_1$ and we have used the fact that

$$\tilde{\beta} = n_1 \cos \theta_1 \tag{3.35}$$

Figure 3.13 shows the ray paths as given by Eq. (3.32) with x_1 = 1.5 m, n_1 = 1.00026 and $k \approx 1.234 \times 10^{-5}$ m^{-1}.

3.4.1 Ray Paths in Parabolic Index Media

We consider a parabolic index medium characterized by the following refractive index distribution:

$$n^2(x) = n_1^2 - \gamma^2 x^2 \tag{3.36}$$

We will use Eq. (3.27) to determine the ray paths. Equation (3.27) can be written as

$$\int \frac{dx}{\sqrt{n^2(x) - \tilde{\beta}^2}} = \pm \frac{1}{\tilde{\beta}} \int dz \tag{3.37}$$

Substituting for $n^2(x)$, we get

$$\int \frac{dx}{\sqrt{x_0^2 - x^2}} = \pm \Gamma \int dz \tag{3.38}$$

where

$$x_0 = \frac{1}{\gamma}\sqrt{n_1^2 - \tilde{\beta}^2} \tag{3.39}$$

and

$$\Gamma = \frac{\gamma}{\tilde{\beta}} \tag{3.40}$$

Writing $x = x_0 \sin \theta$ and carrying out the straightforward integration, we get

$$x = \pm x_0 \sin [\Gamma(z - z_0)] \tag{3.41}$$

We can always choose the origin such that $z_0 = 0$ so that the general ray path would be given by

$$x = \pm x_0 \sin \Gamma z \tag{3.42}$$

We could have also used Eq. (3.28) to obtain the ray path. Now, in an optical waveguide the refractive index distribution is usually written in the form*:

$$\left.\begin{aligned} n^2(x) &= n_1^2\left[1 - 2\Delta\left(\frac{x}{a}\right)\right]^2, \quad |x| < a \text{ core} \\ &= n_2^2 = n_1^2(1 - 2\Delta), \quad |x| < a \text{ cladding} \end{aligned}\right\} \tag{3.43}$$

The region $|x| < a$ is known as the core of the wave guide and the region $|x| > a$ is usually referred to as the cladding. Thus,

$$\gamma = \frac{n_1\sqrt{2\Delta}}{a} \tag{3.44}$$

In a typical parabolic index fiber,

$$n_1 = 1.5, \quad \Delta = 0.01, \quad a = 20\ \mu\text{m} \tag{3.45}$$

giving

$$n_2 \approx 1.485$$

and

$$\gamma \approx 1.0607 \times 10^4\ \text{m}^{-1}$$

Typical ray paths for different values of θ_1 are shown in Fig. 3.23. Obviously, the rays will be guided in the core if $n_2 < \tilde{\beta} < n_1$. When $\tilde{\beta} = n_2$, the ray path will become horizontal at the core-cladding interface. For $\tilde{\beta} < n_2$, the ray will be incident at the core-cladding interface at an angle and the ray will be refracted away. Thus, we may write

* Ray paths in such media are of tremendous importance as they readily lead to very important results for parabolic index fibers which are extensively used in fiber-optic communication systems (see Sec. 27.7).

$$n_2 < \tilde{\beta} < n_1 \quad \Rightarrow \quad \text{Guided rays}$$

$$\tilde{\beta} < n_2 \quad \Rightarrow \quad \text{Refracting rays} \qquad \textbf{(3.46)}$$

In Fig. 3.23, the ray paths shown correspond to

$$z_0 = 0 \quad \text{and} \quad \theta_1 = 4°, 8.13° \text{ and } 20°;$$

the corresponding values of $\tilde{\beta}$ are approximately 1.496 ($> n_2$), 1.485 ($= n_2$) and 1.410 ($< n_2$)—the last ray undergoes refraction at the core–cladding interface. It may be readily seen that the periodical length z_p of the sinusoidal path is given by

$$z_p = \frac{2\pi}{\Gamma} = \frac{2\pi\, a \cos\theta_1}{\sqrt{2\Delta}} \qquad \textbf{(3.47)}$$

Thus, for the two rays shown in Fig. 3.23 (with θ_1 = 4° and 8.13°), the values of z_p would be 0.8864 mm and 0.8796 mm, respectively. Indeed, in the paraxial approximation, $\cos\theta_1 \approx 1$ and all rays have the same periodic length. In Fig. 3.25, we have plotted typical paraxial ray paths for rays launched along the z-axis. Different rays (shown in the figure) correspond to different values of $\tilde{\beta}$.

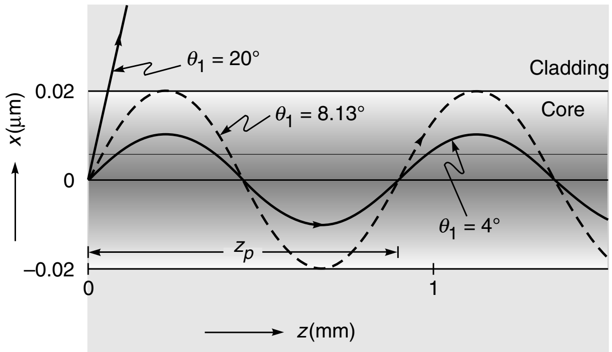

Fig. 3.23 Typical ray paths in a parabolic index medium for parameters given by Eq.(3.45) for θ_1 = 4°, 8.13° and 20°.

Four interesting features may be noted:

(i) In the paraxial approximation ($\tilde{\beta} \approx n_1$) all rays launched horizontally come to a focus at a particular point. Thus the medium acts as a converging lens of focal length given by

$$f \approx \frac{\pi}{2} \frac{a}{\sqrt{2\Delta}} \qquad \textbf{(3.48)}$$

(ii) Rays launched at different angles with the axis (see, for instance, the rays emerging from point P) get trapped in the medium and hence the medium acts like a 'guide'. Indeed such media are referred to as optical waveguides and their study forms a subject of great contemporary interest.

(iii) Ray paths would be allowed only in the region where $\tilde{\beta}$ is less than or equal to $n(x)$ [see Eq. (3.26)]. Further, dx/dz would be zero (i.e., the ray would become parallel to the z-axis) when $n(x)$ equals $\tilde{\beta}$; this immediately follows from Eq. (3.27).

(iv) The rays periodically focus and defocus as shown in Fig. 3.25. In the paraxial approximation, all rays emanating from P will focus at Q and if we refer to our discussion in Example 3.3, all rays must take the same time to go from P to Q. Physically, although the ray PLQ traverses a larger path in comparison to PMQ, it does so in a medium of 'lower' average refractive index—thus the greater path length is compensated for by a greater 'average speed' and hence *all* rays take the same time to propagate through a certain distance of the waveguide (see Sec. 3.4.2 for exact calculation). Therefore, parabolic index waveguides are extensively used in fiber-optic communication systems (see Sec. 28.7).

We may mention here that Gradient-Index GRIN) lenses, characterized by parabolic variation of refractive index in the transverse direction, are now commercially available and find many applications (see Fig. 3.24). For example a GRIN lens can be used to couple the output of a laser diode to an optical fiber; the length of such a GRIN lens would be $z_P/4$ (see Fig. 3.25); typically $z_P \approx$ few cm and the diameter of the lens would be few millimeters. Such small-size lenses find many applications. Similarly, a GRIN lens of length $z_P/2$ can be used to transfer collimated light from one end of the lens to the other.

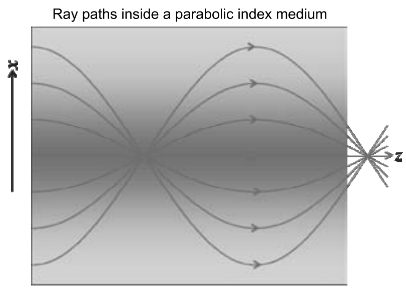

Fig. 3.24 Ray paths in a graded index medium characterized by a refractive index variation which decreases parabolically in the transverse direction. Because of focusing properties, it has many important applications. [*A color photograph of the above figure appears as Fig. 7 in the prelim pages*].

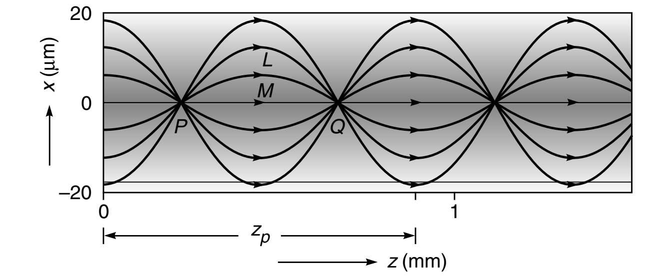

Fig. 3.25 Paraxial ray paths in a parabolic index medium. Notice the periodic focussing and defocussing of the beam.

3.4.2 Transit Time Calculations in a Parabolic Index Waveguide

In this section, we will calculate the time taken by a ray to traverse a certain length through a parabolic index waveguide as described by Eq. (3.36). Such a calculation is of considerable importance in fiber-optic communication systems (see Sec. 28.7). As shown in Sec. 3.4.1, the ray path (inside the core) is given by

$$x = x_0 \sin \Gamma z \tag{3.49}$$

where x_0 and Γ have been defined through Eqs. (3.39) and (3.40). Let $d\tau$ represent the time taken by a ray to traverse the arc length ds [see Fig. 3.12 (b)]:

$$d\tau = \frac{ds}{c/n(x)} \tag{3.50}$$

where c is the speed of light in free space. Since

$$n(x)\frac{dz}{ds} = \tilde{\beta}$$

[see Eq. (3.26)] we may write Eq. (3.50) as

$$d\tau = \frac{1}{c\tilde{\beta}} n^2(x)\, dz$$

$$= \frac{1}{c\tilde{\beta}} [n_1^2 - \gamma^2 x^2]\, dz$$

or

$$d\tau = \frac{1}{c\tilde{\beta}} [n_1^2 - \gamma^2 x_0^2 \sin^2 \Gamma z]\, dz \tag{3.51}$$

where in the last step we have used Eq. (3.49). Thus if $\tau(z)$ represents the time taken by the ray to traverse a distance z along the waveguide, then

$$\tau(z) = \frac{n_1^2}{c\tilde{\beta}}\int_0^z dz - \frac{\gamma^2 x_0^2}{c\tilde{\beta}}\int_0^z \frac{1-\cos(2\Gamma z)}{2}\, dz$$

$$= \frac{1}{c\tilde{\beta}}\left[n_1^2 - \frac{1}{2}\gamma^2 x_0^2\right]z + \frac{\gamma^2 x_0^2}{2c\tilde{\beta}}\frac{1}{2\Gamma}\sin 2\Gamma z$$

or

$$\tau(z) = \frac{1}{2c\tilde{\beta}}[n_1^2 + \tilde{\beta}^2]z + \frac{(n_1^2 - \tilde{\beta}^2)}{4c\gamma}\sin 2\Gamma z \tag{3.52}$$

where we have used Eq. (3.39). When $\tilde{\beta} = n_1$ (which corresponds to the ray along the z-axis)

$$\tau(z) = \frac{z}{c/n_1} \tag{3.53}$$

This is what we should have expected as the ray will *always* travel with speed c/n_1. For large values of z, the second term on the RHS of Eq. (3.52) would make a negligible contribution to $\tau(z)$ and we may write

$$\tau(z) \approx \frac{1}{2c}\left[\tilde{\beta} + \frac{n_1^2}{\tilde{\beta}}\right]z \tag{3.54}$$

Now, if a pulse of light is incident on one end of the waveguide, it would, in general, excite all rays and since different rays take different amounts of time, the pulse will get temporally broadened. Thus, for a parabolic index waveguide, this broadening will be given by

$$\Delta\tau = \tau(\tilde{\beta} = n_2) - \tau(\tilde{\beta} = n_1)$$

or

$$\Delta\tau = \frac{z}{2c}\frac{(n_1 - n_2)^2}{n_2} \approx \frac{zn_2}{2c}\Delta^2 \tag{3.55}$$

where in the last step we have assumed

$$\Delta \equiv \frac{n_1^2 - n_2^2}{2n_1^2} \approx \frac{n_1 - n_2}{n_2} \tag{3.56}$$

For the fiber parameters given by Eq. (3.45), we get

$$\Delta\tau \approx 0.25 \text{ ns/km} \tag{3.57}$$

We will use this result in Chapter 28.

Example 3.9 We next consider the ray paths in a medium characterized by the following refractive index variation:

$$n^2(x) = n_1^2 \qquad x < 0$$

$$= n_1^2 - gx \qquad x > 0 \tag{3.58}$$

Thus, in the region $x > 0$, $n^2(x)$ decreases linearly with x and Eq. (3.28) takes the form

$$\frac{d^2x}{dz^2} = -\frac{g}{2\tilde{\beta}^2}$$

The general solution of which is given by

$$x(z) = -\frac{g}{4\tilde{\beta}^2}z^2 + K_1 z + K_2 \quad \textbf{(3.59)}$$

Consider a ray incident on the origin ($x = 0$, $z = 0$) as shown in Fig. 3.26. Thus,

$$K_2 = 0 \quad \text{and} \quad \tilde{\beta} = n_1 \cos\theta_1 \quad \textbf{(3.60)}$$

Further,

$$\left.\frac{dx}{dz}\right|_{z=0} = K_1 = \tan\theta_1 \quad \textbf{(3.61)}$$

Thus the ray path will be given by

$$x(z) \left.\begin{aligned} &= (\tan\theta_1)z && z < 0 \\ &= -\frac{gz}{4\tilde{\beta}^2}(z - z_0) && 0 < z < z_0 \\ &= -\frac{gz_0}{4\tilde{\beta}^2}(z - z_0) && z > z_0 \end{aligned}\right\} \quad \textbf{(3.62)}$$

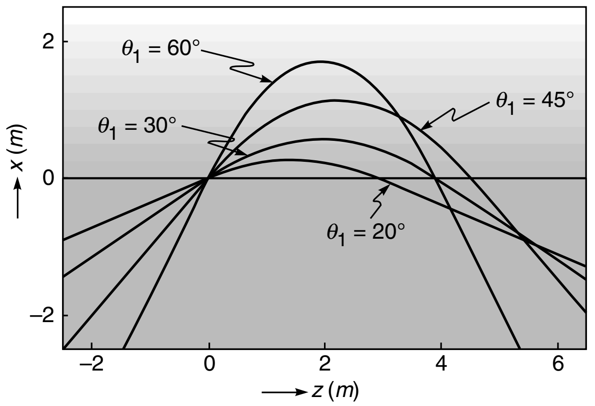

Fig. 3.26 Parabolic ray paths (corresponding to θ_1 = 20°, 30°, 45° and 60°) in a medium characterized by refractive index variation given by Eq. (3.58). The ray paths in the region $x < 0$ are straight lines.

where

$$z_0 = \frac{2n_1^2}{g}\sin 2\theta_1$$

Thus, in the region $0 < z < z_0$, the ray path is a parabola. Typical ray paths are shown in Fig. 3.26, the calculations correspond to

$$n_1 = 1.5, \quad g = 0.1\ \text{m}^{-1}$$

and different rays correspond to

$$\theta_1 = \frac{\pi}{9}, \frac{\pi}{6}, \frac{\pi}{4} \text{ and } \frac{\pi}{3}$$

3.4.3 Reflections from the Ionosphere

The ultraviolet rays in the solar radiation result in the ionization of the constituent gases in the atmosphere resulting in the formation of what is known as the ionosphere. The ionization is almost negligible below a height of about 60 km. Because of the presence of the free electrons (in the ionosphere), the refractive index is given by [see Eq. (7.76)]:

$$n^2(x) = 1 - \frac{N_e(x)\,q^2}{m\varepsilon_0\omega^2} \quad \textbf{(3.63)}$$

where

$N_e(x)$ represents the number of electrons/unit volume in m^{-3}

x represents the height above the ground in meters

ω represents the angular frequency of the electromagnetic wave

$q \approx 1.60 \times 10^{-19}$ C represents the charge of the electron

$m \approx 9.11 \times 10^{-31}$ kg represents the mass of the electron, and

$\varepsilon_0 \approx 8.854 \times 10^{-12} \times 10^{-12}\ \text{C}^2/\text{N–m}^2$ represents the dielectric permittivity of vacuum

Thus, as the electron density starts increasing from 0 (beyond the height of 60 km) the refractive index starts decreasing and the ray paths would be similar to that described in Example 3.9.

If n_T represents the refractive index at the turning point (where the ray becomes horizontal) then (see Fig. 3.27)

$$\tilde{\beta} = \cos\theta_1 = n_T \quad \textbf{(3.64)}$$

Thus if an electromagnetic signal is sent from the point A (at an angle θ_1) is received at the point B, one can determine the refractive index (and hence the electron density) of the ionospheric layer where the beam has undergone the reflection. This is how the short-wave radio broadcasts ($\lambda \approx$ 20 m) sent at a particular angle from a particular city (say London) would reach another city (say New Delhi) after undergoing reflection from the ionosphere. Further, for normal incidence, $\theta = \pi/2$ and $n_T = 0$ implying

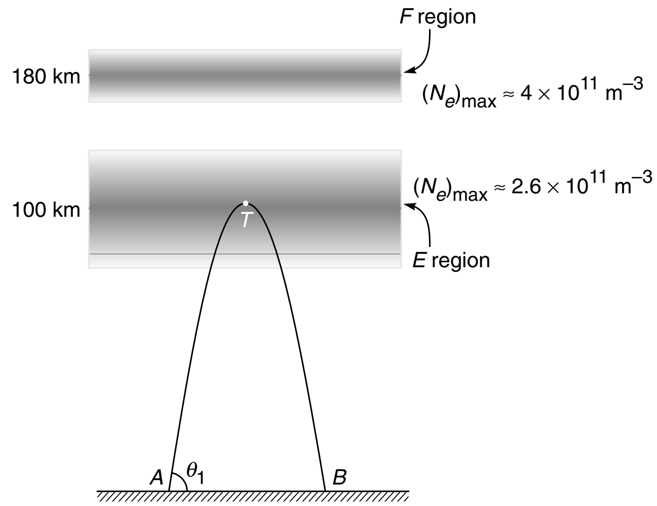

Fig. 3.27 Reflection from the E region of the ionosphere. The point T represents the turning point. The shading shows the variation of electron density.

$$N_e(x_T) = \frac{m\varepsilon_0 \omega^2}{q^2} \tag{3.65}$$

In a typical experiment, an electromagnetic pulse (of frequency between 0.5 and 20 MHz) is sent vertically upwards and if the echo is received after a delay of Δt seconds, then

$$\Delta t \approx \frac{2h}{c} \tag{3.66}$$

where h represents the height at which it undergoes reflection. Thus, if electromagnetic pulse is reflected from the E layer of ionosphere (which is at a height of about 100 km), the echo will be received after about 670 μs. Alternatively, by measuring the delay Δt, one can determine the height (at which the pulse gets reflected) from the following relation

$$h \approx \frac{c}{2}\Delta t \tag{3.67}$$

In Fig. 3.28, we have plotted the frequency dependence of the equivalent height of reflection (as obtained from the delay time of echo) from the E and F regions of the ionosphere. From the figure we find that at $\nu = 4.6 \times 10^6$ Hz, echoes suddenly disappear from the 100 km height. Thus,

$$N_e(100 \text{ km}) \approx \frac{m\varepsilon_0 (2\pi\nu)^2}{q^2}$$

$$\approx \frac{9.11\times 10^{-31} \times 8.854 \times 10^{-12} \times (2\pi \times 4.6 \times 10^6)^2}{(1.6 \times 10^{-19})^2}$$

$$\approx 2.6 \times 10^{11} \text{ electrons/m}^3$$

If we further increase the frequency, the echoes appear from the F region of the ionosphere. For more details of the studies on the ionosphere, the reader is referred to one of the most outstanding texts on the subject by Professor S. K. Mitra [Ref. 3.9].

Example 3.10 In this example, we will obtain the solution of the ray equation for the refractive index variation given by

$$n^2(x) = n_0^2 + n_2^2(1 - e^{-\alpha x}) \tag{3.68}$$

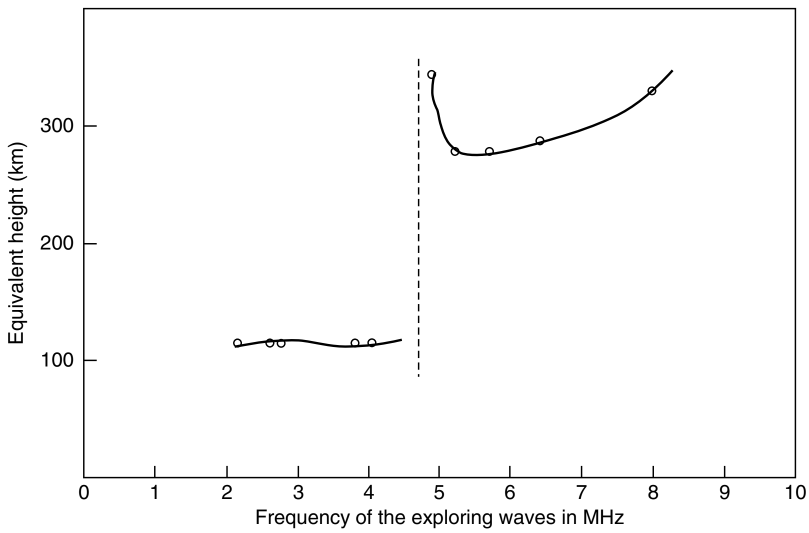

Fig. 3.28 Frequency dependence of the equivalent height of reflection from the E and F regions of the ionosphere. [*Adapted from Ref. 3.9*].

Substituting in Eq. (3.27), we would obtain

$$\pm dz = \frac{\tilde{\beta}\, dx}{\left[(n_0^2 + n_2^2 - \tilde{\beta}^2) - n_2^2\, e^{-\alpha x}\right]^{1/2}}$$

$$= \frac{\tilde{\beta}\, e^{\alpha x/2}\, dx}{n_2\,[K^2 e^{\alpha x} - 1]^{1/2}}$$

or
$$\pm dz = \frac{2\tilde{\beta}}{K\,\alpha n_2} \frac{d\Phi}{(\Phi^2 - 1)^{1/2}} \tag{3.69}$$

where
$$K = \frac{1}{n_2}(n_0^2 + n_2^2 - \tilde{\beta}^2)^{1/2} \tag{3.70}$$

and
$$\Phi(x) = K\, e^{\alpha x/2} \tag{3.71}$$

The + and – sign in Eq. (3.69) correspond to a ray going up and a ray going down respectively. Further,

$$\tilde{\beta} = n_1 \cos \theta_1 \tag{3.72}$$

where θ_1 is the angle that the ray initially makes with the z-axis at $x = x_1$, $z = 0$ and $n_1 = n(x_1)$. Carrying out the elementary integration, we get

$$x(z) = \frac{2}{\alpha} \ln\left[\frac{1}{K} \cosh \gamma (C \pm z)\right] \tag{3.73}$$

where
$$\gamma = \frac{\alpha\, K\, n_2}{2\tilde{\beta}} \tag{3.74}$$

which gives us the ray path. Since $x = x_1$ at $z = 0$ (the initial point)

$$C = \frac{1}{\gamma} \cosh^{-1}(K e^{\alpha x_1/2}) \tag{3.75}$$

Further,

$$K e^{\alpha x_1/2} = \left[\frac{n_0^2 + n_p^2 - \tilde{\beta}^2}{n_0^2 + n_p^2 - n_1^2}\right]^{1/2} \tag{3.76}$$

Thus for a ray launched horizontally at $x = x_1$, $C = 0$. Typically ray paths (for different values of θ_1) are shown in Figs. 3.14 and 3.15.

3.5 REFRACTION OF RAYS AT THE INTERFACE BETWEEN AN ISOTROPIC MEDIUM AND AN ANISOTROPIC MEDIUM

LO 5

In this section, we will use Fermat's principle to determine the direction of the refracted ray for a ray incident at the interface of an isotropic and an anisotropic medium*. We may point out that in an isotropic medium the properties remain the same in all directions; typical examples are glass, water and air. On the other hand, in an anisotropic medium, some of the properties (such as speed of light) may be different in different directions. In Chapter 22, we will consider anisotropic media in greater detail; we may mention here that when a light ray is incident on a crystal like calcite, it (in general) splits into two rays known as ordinary and extraordinary rays. The velocity of the ordinary ray is the same in all directions. Thus the ordinary ray obeys Snell's laws but the extraordinary ray does not. We will now use Fermat's principle to study the refraction of a ray when it is incident from an isotropic medium into an anisotropic medium—both media are assumed to be homogeneous.

In a uniaxial medium, the refractive index variation for the extraordinary ray is given by [see Eq. (22.121)]

$$n^2(\theta) = n_o^2 \cos^2 \theta + n_e^2 \sin^2 \theta \tag{3.77}$$

where n_o and n_e are constants of the crystal and θ represents the angle that the ray makes with the optic axis. Obviously, when the extraordinary ray propagates parallel to the optic axis (i.e., when $\theta = 0$), its speed is c/n_o and when it propagates perpendicular to the optic axis ($\theta = \pi/2$) its speed is c/n_e.

3.5.1 Optic Axis Normal to the Surface

We first consider the particularly simple case of the optic axis being normal to the surface. Referring to Fig. 3.29, the optical path length from A and B is given by

$$L_{\text{op}} = n_1[h_1^2 + (L - x)^2]^{1/2} + n(\theta)[h_2^2 + x^2]^{1/2} \tag{3.78}$$

where n_1 is the refractive index of medium I and we have assumed the incident ray, the refracted ray and the optic axis to lie in the same plane. Since

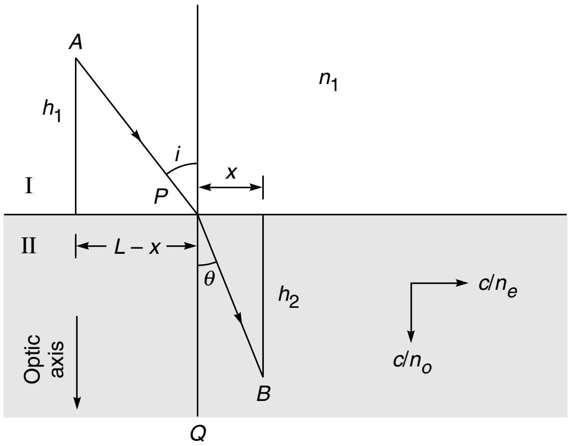

Fig. 3.29 The direction of the refracted extraordinary ray when the optic axis (of the uniaxial crystal) is normal to the surface.

* A proof for the applicability of Fermat's principle in anisotropic media has been given by Newcomb (Ref. 3.10); the proof, however, is quite complicated. Ray paths in biaxial media are discussed in Ref. 3.11.

$$\cos\theta = \frac{h_2}{(h_2^2 + x^2)^{1/2}} \quad \text{and} \quad \sin\theta = \frac{x}{(h_2^2 + x^2)^{1/2}}$$

we have

$$L_{op} = n_1\,[h_1^2 + (L - x)]^{1/2} + [n_o^2 h_2^2 + n_e^2 x^2]^{1/2} \tag{3.79}$$

For the actual ray path, we must have

$$\frac{dL_{op}}{dx} = 0$$

implying

$$\frac{n_1(L-x)}{[h_1^2 + (L-x)^2]^{1/2}} = \frac{n_e^2 x}{\left[n_o^2 h_2^2 + n_e^2 x^2\right]^{1/2}}$$

or

$$n_1 \sin i = \frac{n_e^2 \tan r}{\left[n_o^2 + n_e^2 \tan^2 r\right]^{1/2}} \tag{3.80}$$

where we have used the fact that the

angle of refraction $r = \theta$ and $\tan r = \dfrac{x}{h_2}$.

Simple manipulations give us

$$\tan r = \frac{n_o n_1 \sin i}{n_e \sqrt{n_e^2 - n_1^2 \sin^2 i}} \tag{3.81}$$

using which we can calculate the angle of refraction for a given angle of incidence (when the optic axis is normal to the surface). As a simple example, we assume the first medium to be air so that $n_1 = 1$. Then

$$\tan r = \frac{n_o \sin i}{n_e \sqrt{n_e^2 - \sin^2 i}} \quad (\text{when } n_1 = 1) \tag{3.82}$$

If we assume the second medium to be calcite, then

$$n_o = 1.65836, \quad \text{and} \quad n_e = 1.48641$$

Thus for $i = 45°$, we readily get

$$r \approx 31.1°$$

It may be seen that if $n_o = n_e = n_2$ (say) then Eq. (3.80) simplifies to

$$n_1 \sin i = n_2 \sin r \tag{3.83}$$

which is nothing but Snell's law.

3.5.2 Optic Axis in the Plane of Incidence*

We next consider a more general case of the optic axis making an angle ϕ with the normal; however, the optic axis is assumed to lie in the plane of incidence as shown in Fig. 3.30. We may mention here that in general, in an anisotropic medium, the refracted ray does not lie in the plane of incidence. However, it can be shown that if the optic axis lies in the plane of incidence then the refracted ray also lies in the plane of incidence. In the present calculation, we are assuming this and finding the direction of the refracted ray for a given angle of incidence. Now, the optical path length from A to B (see Fig. 3.30) is given by

$$L_{op} = n_1[h_1^2 + (L-x)^2]^{1/2} + n(\theta)[h_2^2 + x^2]^{1/2} \tag{3.84}$$

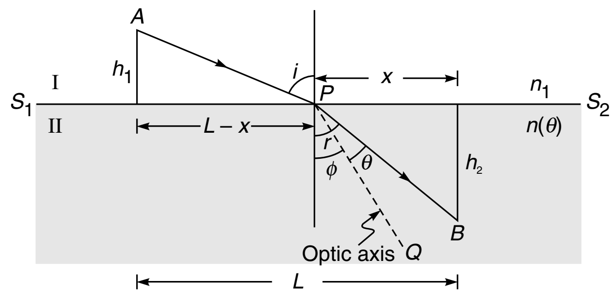

Fig. 3.30 The direction of the refracted extraordinary ray when the optic axis (of the uniaxial crystal) lies in the plane of incidence making an angle ϕ with the normal to the interface.

Since $\theta = r - \phi$, we have

$$n^2(\theta) = n_o^2 \cos^2 (r - \phi) + n_e^2 \sin^2 (r - \phi)$$

$$= n_o^2 (\cos r \cos \phi + \sin r \sin \phi)^2 + n_e^2 (\sin r \cos \phi - \cos r \sin \phi)^2$$

$$= n_o^2 \left[\frac{h_2}{\sqrt{h_2^2 + x^2}} \cos\phi + \frac{x}{\sqrt{h_2^2 + x^2}} \sin\phi\right]^2 + n_e^2 \left[\frac{x}{\sqrt{h_2^2 + x^2}} \cos\phi - \frac{h_2}{\sqrt{h_2^2 + x^2}} \sin\phi\right]^2$$

Thus,

$$n(\theta) = \frac{1}{\sqrt{h_2^2 + x^2}}\, [n_o^2 (h_2 \cos\phi + x \sin\phi)^2 + n_e^2 (x \cos\phi - h_2 \sin\phi)^2]^{1/2} \tag{3.85}$$

and

$$L_{op} = n_1[h_1^2 + (L - x)^2]^{1/2} + [n_o^2 (h_2 \cos\phi + x \sin\phi)^2 + n_e^2 (x \cos\phi - h_2 \sin\phi)^2]^{1/2} \tag{3.86}$$

* May be skipped in the first reading.

For the actual ray path, we must have

$$\frac{dL_{op}}{dx} = 0$$

implying

$$\frac{n_1 (L - x)}{[h_1^2 + (L - x)^2]^{1/2}} =$$

$$\frac{n_o^2 (h_2 \cos\phi + x \sin\phi) \sin\phi + n_e^2 (x \cos\phi - h_2 \sin\phi) \cos\phi}{[n_o^2 (h_2 \cos\phi + x \sin\phi)^2 + n_e^2 (x \cos\phi - h_2 \sin\phi)^2]^{1/2}}$$

or $$n_1 \sin i = \frac{n_o^2 \cos\theta \sin\phi + n_e^2 \sin\theta \cos\phi}{[n_o^2 \cos^2\theta + n_e^2 \sin^2\theta]^{1/2}} \quad \textbf{(3.87)}$$

For given values of the angles i and ϕ, the above equation can be solved to give the values of θ and hence the angle of refraction r (= $\theta + \phi$).

Some interesting particular cases may be noted.

(i) When $n_o = n_e = n_2$, the anisotropic medium becomes isotropic and Eq. (3.87) simplifies to

$$n_1 \sin i = n_2 \sin(\theta + \phi) = n_2 \sin r$$

which is nothing but Snell's law.

(ii) When $\phi = 0$, i.e., the optic axis is normal to the surface, Eq. (3.87) becomes

$$n_1 \sin i = \frac{n_e^2 \sin\theta}{[n_o^2 \cos^2\theta + n_e^2 \sin^2\theta]^{1/2}}$$

$$= \frac{n_e^2 \sin r}{[n_o^2 \cos^2 r + n_e^2 \sin^2 r]^{1/2}} \quad \textbf{(3.88)}$$

where we have used the fact that $r = \theta$. The above equation is identical to Eq. (3.80).

(iii) Finally, we consider normal incidence, i.e., $i = 0$. Thus, Eq. (3.87) gives us

$$n_o^2 \cos\theta \sin\phi + n_e^2 \sin\theta \cos\phi = 0$$

or

$$n_o^2 \cos(r - \phi) \sin\phi + n_e^2 \sin(r - \phi) \cos\phi = 0$$

or

$$\cos r\, [n_o^2 \cos\phi \sin\phi - n_e^2 \sin\phi \cos\phi] + \sin r\, [n_o^2 \sin^2\phi + n_e^2 \cos^2\phi] = 0$$

or

$$\tan r = \frac{(n_e^2 - n_o^2) \sin\phi \cos\phi}{n_o^2 \sin^2\phi + n_e^2 \cos^2\phi} \quad \textbf{(3.89)}$$

Equation (3.89) shows that in general $r \neq 0$ (see Fig. 3.31). We may mention here that, for normal incidence, the above analysis is valid for an arbitrary orientation of the optic axis; the refracted (extraordinary) ray lies in the plane containing the normal and the optic axis. Furthermore, for normal incidence, when the crystal is rotated about the normal, the refracted ray also rotates on the surface of a cone [see Fig. 22.16(b)].

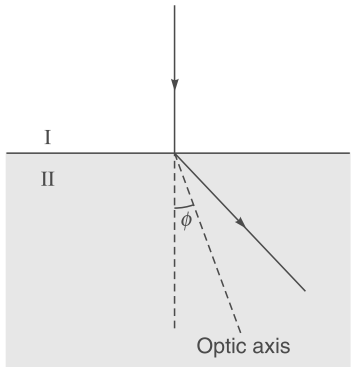

Fig. 3.31 For normal incidence, in general, the refracted extraordinary ray undergoes finite deviation. However, the ray proceeds undeviated when the optic axis is parallel or normal to the surface.

Reverting to Eq. (3.89) we note that when the optic axis is normal to the surface ($\phi = 0$) or when the optic axis is parallel to the surface but lying in the plane of incidence ($\phi = \pi/2$), $r = 0$ and the ray goes undeviated.

Summary

- The slightly modified version of Fermat's principle is, *the actual ray path between two points is the one for which the optical path length is stationary with respect to variations of the path.*
- Laws of reflections and Snell's law of refraction ($n_1 \sin\phi_1 = n_2 \sin\phi_2$, where ϕ_1 and ϕ_2 represent the angles of incidence and refraction) can be derived from Fermat's principle.
- For an inhomogeneous medium characterized by the refractive index variation $n(x)$, the ray paths [$x(z)$] are such that the product $n(x)\cos\theta(x)$ remains constant, here $\theta(x)$ is the angle that the ray makes with the z-axis; this constant is denoted by $\tilde{\beta}$ which is known as the ray invariant. The exact ray paths are determined by solving either of the equations:

$$\frac{dx}{dz} = \pm \frac{\sqrt{n^2(x) - \tilde{\beta}^2}}{\tilde{\beta}}$$

or $$\frac{d^2x}{dz^2} = \frac{1}{2\tilde{\beta}^2} \frac{dn^2(x)}{dx}$$

where the invariant $\tilde{\beta}$ is determined from the initial launching condition of the ray.

- Ray paths obtained by solving the ray equation can be used to study mirage, looming and also reflections from the ionosphere.
- Continuous variation is observed in refractive index in an inhomogeneous medium whereas it is constant at every place in homogeneous medium.
- In the paraxial approximation, cos theta is equal to one and all rays have the same periodic length.
- In a parabolic index medium $n^2(x) = n_1^2 - \gamma^2 x^2$, the ray paths are sinusoidal:

$$x(z) = \pm x_0 \sin \Gamma z$$

where $\Gamma = \frac{1}{\tilde{\beta}}$, $x_0 = \frac{1}{\gamma}\sqrt{n_1^2 - \tilde{\beta}^2}$ and we have assumed $z = 0$ where $x = 0$. Rays launched at different angles take approximately the same time in propagating through a large length of the medium.
- Fermat's principle can be used to study refraction of rays at the interface of an isotropic medium and an anisotropic medium.
- Speed of an extraordinary ray travelling parallel to optic axis is c/n_0 whereas it is c/n_e when it propagates perpendicularly.

Problems

In the first three problems, we will use Fermat's principle to derive laws governing paraxial image formation by spherical mirrors.

3.1 Consider an object point O in front of a concave mirror whose center of curvature is at the point C. Consider an arbitrary point Q on the axis of the system and using a method similar to that used in Example 3.3, show that the optical path length L_{op} (= $OS + SQ$) is approximately given by

$$L_{op} \approx x + y + \frac{1}{2}r^2\left[\frac{1}{x} + \frac{1}{y} - \frac{2}{r}\right]\theta^2 \tag{3.90}$$

where the distances x, y and r and the angle θ are defined in Fig. 3.32; θ is assumed to be small. Determine the paraxial image point and show that the result is consistent with the mirror equation

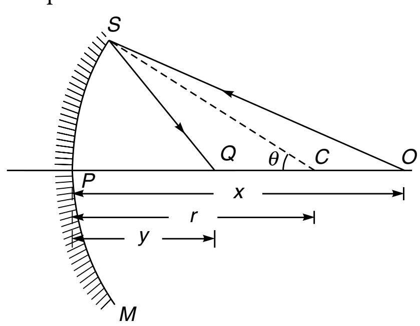

Fig. 3.32 Paraxial image formation by a concave mirror.

$$\frac{1}{u} + \frac{1}{v} = \frac{2}{R} \tag{3.91}$$

where u and v are the object and image distance and R is the radius of curvature with the sign convention that all distances to the right of P are positive and to its left negative.

3.2 Fermat's principle can also be used to determine the paraxial image points when the object forms a virtual image. Consider an object point O in front of the convex mirror SPM (see Fig. 3.33). Assume the optical path length L_{op} to be $OS - SQ$; the minus sign occurs because the rays at S point away from Q (see Example 3.4). Show that

$$L_{op} \approx OS - SQ \approx x - y + \frac{1}{2}r^2\left[\frac{1}{x} - \frac{1}{y} + \frac{2}{r}\right]\theta^2 \tag{3.92}$$

where the distances x, y and r and the angle θ are defined in Fig. 3.33. Show that the paraxial image is formed at $y = y_0$ which is given by

$$\frac{1}{x} - \frac{1}{y_0} = -\frac{2}{r} \tag{3.93}$$

and is consistent with Eq. (3.91). [Which the object distance u is positive, the image distance v and the radius of curvature R are negative since the image point and the center of curvature lie on the left of the point P.]

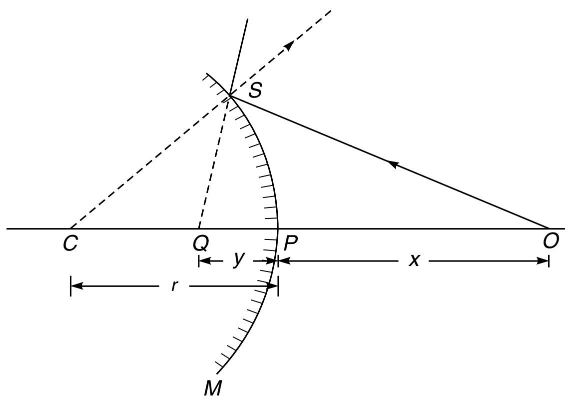

Fig. 3.33 Paraxial image formation by a convex mirror.

3.3 Use Fermat's principle to determine the mirror equation for an object point at a distance less than $R/2$ from a concave mirror of radius of curvature R.

3.4 Consider a point object O in front of a concave refracting surface SPM separating two media of refracting indices n_1 and n_2 (see Fig. 3.34); C represents the center of curvature. In this case also one obtains a virtual image. Let Q represent an arbitrary point on the axis. We now have to consider the optical path length $L_{op} = n_1\, OS - n_2\, SQ$; show that it is given by

$$L_{op} = n_1\, OS - n_2\, SQ$$

$$\approx n_1 x - n_2 y - \frac{1}{2} r^2\left[\frac{n_2}{y} - \frac{n_1}{x} - \frac{n_2 - n_1}{r}\right]\theta^2 \tag{3.94}$$

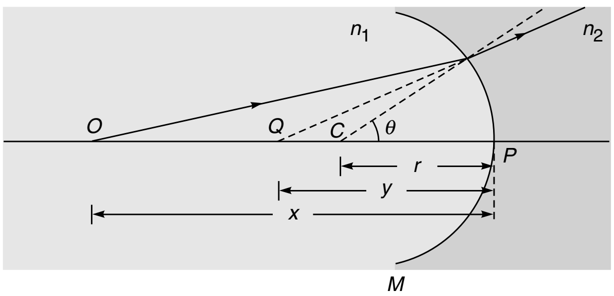

Fig. 3.34 Paraxial image formation by a concave refracting surface *SPM*.

Also show that the above expression leads to the paraxial image point which is consistent with Eq. (3.10); we may note that u, v and R are all negative quantities because they are on the left of the refracting surface.

3.5 If we rotate an ellipse about its major axis we obtain what is known as an ellipsoid of revolution. Show by using Fermat's principle that all rays parallel to the major axis of the ellipse will focus to one of the focal points of the ellipse (see Fig. 3.35), provided the eccentricity of the ellipse equals n_1/n_2.

[**Hint:** *Start with the condition that*

$$n_2\, AC' = n_1\, QB + n_2\, BC$$

and show that the point B (whose coordinates are x and y) lies on the periphery of an ellipse].

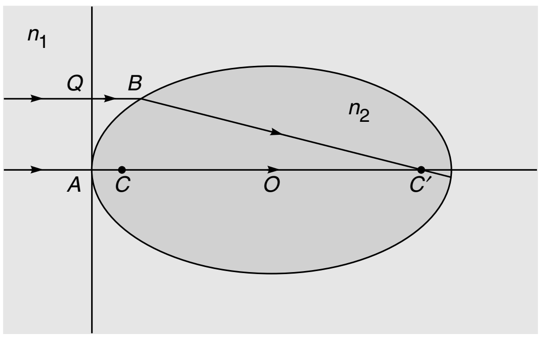

Fig. 3.35 All rays parallel to the major axis of the ellipsoid of revolution will focus to one of the focal points of the ellipse provided the eccentricity = n_1/n_2.

3.6 C is the center of the reflecting sphere of radius R (see Fig. 3.36). P_1 and P_2 are two points on a diameter equidistant from the center. **(a)** Obtain the optical path length $P_1O + OP_2$ as a function of θ, and **(b)** find the values of θ for which P_1OP_2 is a ray path from reflection at the sphere.

3.7 *SPM* is a spherical refracting surface separating two media of refractive indices n_1 and n_2. (see Fig. 3.35). Consider an object point O forming a virtual image at the point I. We assume that *all* rays emanating from O appear to emanate from I so as to form a perfect image. Thus, according to Fermat's principle, we must have

$$n_1\, OS - n_2\, SI = n_1\, OP - n_2\, PI$$

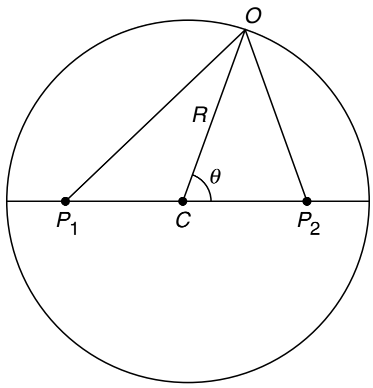

Fig. 3.36 A spherical reflector.

where S is an arbitrary point on the refracting surface. Assuming the right-hand side to be zero, show that the refracting surface is spherical, with the radius given by

$$r = \frac{n_1}{n_1 + n_2}\, OP \tag{3.95}$$

Thus show that

$$n_1^2 d_1 = n_2^2 d_2 = n_1 n_2 r \tag{3.96}$$

where d_1 and d_2 are defined in Fig. 3.37. (see also Fig. 4.12 and Sec. 4.10).

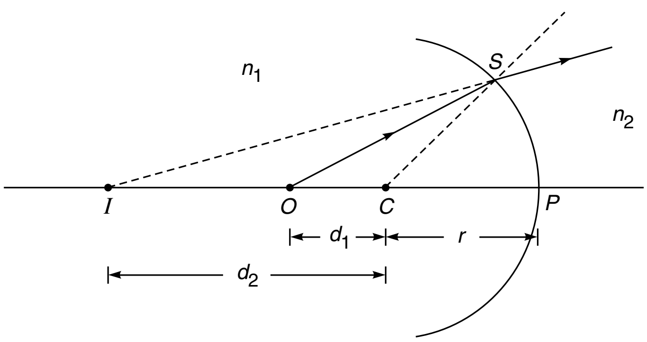

Fig. 3.37 All rays emanating from O and getting refracted by the spherical surface *SPM* appear to come from I.

[**Hint:** *We consider a point C which is at a distance d_1 from the point O and d_2 from the point I. Assume the origin to be at O and let (x, y, z) represent the coordinates of the point S. Thus,*

$$n_1\,(x^2+y^2+z^2)^{1/2} - n_2\,(x^2+y^2+\Delta^2)^{1/2}$$

$$= n_1\,(r+d_1) - n_2\,(r+d_2) = 0$$

where $\Delta = d_2 - d_1$. The above equation would give the equation of a sphere whose center is at a distance of $n_2 r/n_1$ ($= d_1$) from O.]

3.8 Referring to Fig. 3.38, if I represents a perfect image of the point O, show that the equation of the refracting surface (separating two media of refractive indices n_1 and n_2) is given by

$$n_1\,[x^2+y^2+z^2]^{1/2} + n_2\,[x^2+y^2+(z_2-z)^2]^{1/2}$$

$$= n_1 z_1 - n_2 (z_2 - z_1) \tag{3.97}$$

where the origin is assumed to be at the point O and the coordinates of P and I are assumed to be $(0,0,z_1)$ and $(0,0,z_2)$ respectively. The surface corresponding to Eq. (3.97) is known as a Cartesian oval.

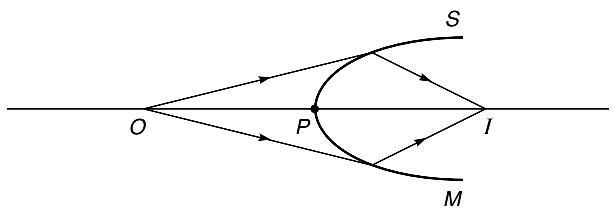

Fig. 3.38 The Cartesian oval. All rays emanating from O and getting refracted by SPM pass through I.

3.9 For the refractive index variation given by Eqs. (3.21) and (3.22), a ray is launched at $x = 0.43$ m making an angle $-\pi/60$ with the z-axis (see Fig. 3.14). Calculate the value of x at which it will become horizontal. [**Ans:** $x \approx 0.41$ m]

3.10 For the refractive index variation given by Eqs. (3.21) and (3.22), a ray is launched at $x = 2.8$ m such that it becomes horizontal at $x = 0.2$ m (see Fig. 3.15). Calculate the angle that the ray will make with the z-axis at the launching point.

[**Ans:** $\theta_1 \approx 19°$]

3.11 Consider a parabolic index medium characterized the following refractive index variation:

$$n^2(x) = n_1^2\left[1 - 2\Delta\left(\frac{x}{a}\right)^2\right] \qquad |x| < a$$

$$= n_1^2(1-2\Delta) = n_2^2 \quad |x| > a$$

Assume $n_1 = 1.50$, $n_2 = 1.48$, $a = 50\ \mu$m. Calculate the value of Δ.

(a) Assume rays launched on the axis at $z = 0$ (i.e., $x = 0$ when $z = 0$) with

$\tilde{\beta}$ = 1.495, 1.490, 1.485, 1.480, 1.475 and 1.470

In each case, calculate the angle that the ray initially makes with the z-axis (θ_1) and plot the ray paths. In each case, find the height at which the ray becomes horizontal.

(b) Assume-rays incident normally on the plane $z = 0$ at $x = 0$, $\pm 10\ \mu$m, ± 20 mm, $\pm 30\ \mu$m, and $\pm 40\ \mu$m. Find the corresponding values of $\tilde{\beta}$, calculate the focal length for each ray and qualitatively plot the ray paths.

3.12 In an inhomogeneous medium the refractive index is given by

$$n^2(x) = 1 + \frac{x}{L} \qquad \text{for } x > 0$$

$$= 1 \qquad \text{for } x < 0$$

Write down the equation of a ray (in the x–z plane) passing through the point (0, 0, 0) where its orientation with respect to x-axis is 45°.

$$\left[\textbf{Ans: } x(z) = \frac{z^2}{4L\tilde{\beta}^2} + z\right]$$

3.13 For the refractive index profile given by Eq. (3.23), show that Eq. (3.27) can be written in the form

$$\pm\frac{\alpha K_1 n_2}{2\tilde{\beta}}\,dz = \frac{dG}{\sqrt{1-G^2}} \tag{3.98}$$

where

$$K_1 = \frac{\sqrt{\tilde{\beta}^2 - n_0^2}}{n_2} \quad \text{and} \quad G(x) = K_1\,e^{-\alpha x/2} \tag{3.99}$$

Integrate Eq. (3.98) to determine the ray paths.

3.14 Consider a graded index medium characterized by the following refractive index distribution:

$$n^2(x) = n_1^2\,\text{sech}^2\,gx \tag{3.100}$$

Substitute in Eq. (3.27) and integrate to obtain

$$x(z) = \frac{1}{g}\sinh^{-1}\left[\frac{\sqrt{n_1^2-\tilde{\beta}^2}}{\tilde{\beta}}\sin gz\right] \tag{3.101}$$

Note that the periodic length

$$z_p = \frac{2\pi}{g}$$

is independent of the launching angle (see Fig. 3.39) and *all* rays rigorously take the same amount of time in propagating through a distance z_p in the z-direction.

[**Hint:** *While carrying out the integration, make the substitution*: $\zeta = \frac{\tilde{\beta}}{\sqrt{n_1^2-\tilde{\beta}^2}}\sinh gx$]

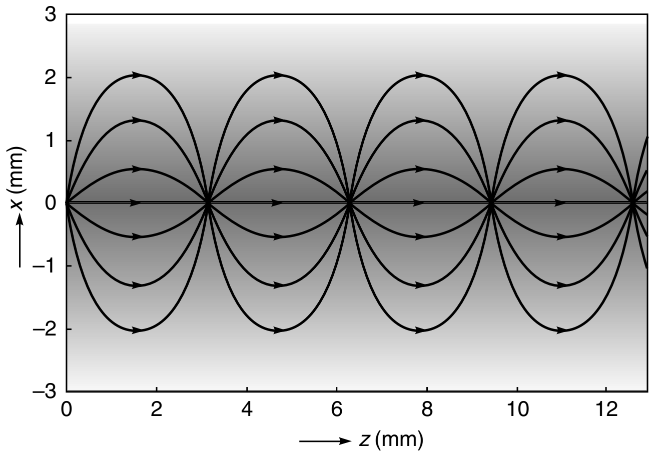

Fig. 3.39 Ray paths in a graded index medium characterized by Eq. (3.100).